Synthesis, Spectroscopic characterization, electrochemical behavior and biological activity of Some Phosphine Schiff Base Complexes.

A.M. A. Alaghaz[a,c], Ahmed I. Hanafy [*b,c]

a Chemistry Department, Faculty of Science, Jazan University, Saudi Arabia.
b Chemistry Department, Faculty of Science, Taif University, Saudi Arabia.
c permanent address; Chemistry Department, Faculty of Science, Al-Azhar
University, Cairo, Egypt.
*Corresponding authors; ahmedih@yahoo.com (A.I. Hanafy).

Abstract : The phosphine Schiff base 4-((Z)-(4-bromophenylimino)(diphenyl-phosphino)methyl)benzene-1,2,3-triol (H_3L), and its Cu(II), Cd(II), Ti(III), Cr(III), Mn(III), Fe(III), MoO_2(VI), and UO_2(VI) complexes **(1-8)**, respectively, have been prepared. The structure of the ligand and its complexes were investigated using elemental analysis, FT-IR, UV/Visible, EPR, ^{13}C, and ^{31}P-NMR, magnetic susceptibility, and conductance measurements. The ligand H_3L behaves as a bidentate ligand in which the oxygen atom in the *ortho* position and methine nitrogen atoms of the ligand coordinate to the metal ions. The keto-enol tautomeric forms of the phosphine Schiff base ligand H_3L have been investigated in polar and non-polar organic solvents. All metal ions form complexes in mole ratio of 1 : 2 metal : ligand. The solid state dc electrical conductivity of the ligand and its complexes have been measured over 315-405 K, and the complexes were found to be of semiconducting nature. The antibacterial and antifungal activities of the ligand and its metal complexes have been investigated. Some of these metal complexes showed significant activity against Pseudomonas and Klebsiella bacteria and two fungi (A. Niger and A. Flavous).
[A.M. A. Alaghaz, Ahmed I. Hanafy. Synthesis, Spectroscopic characterization, electrochemical behavior and biological activity of Some Phosphine Schiff Base Complexes. Journal of American Science 2011; 7(12):971-9].
(ISSN: 1545-1003). http://www.americanscience.org.

1. Introduction

The synthesis of Schiff bases and their coordination chemistry have been reported and considered as a subject of intensive study[1-3] Schiff base complexes have been amongst the most widely studied coordination compounds in the past few years, since they are becoming increasingly important as biochemical, analytical and antimicrobial reagents [4,5]. It has been shown that Schiff base complexes derived from 4-hydroxy-salicylaldehyde and amines have strong anticancer activity, e.g., against *Ehrlich ascites carcinoma* (EAC) [6]. It is well known that some drugs have greater activity when administered as metal complexes than that of the free organic compounds [7]. Phosphate and phosphine Schiff bases have been prepared and fully characterized [8]. Organic phosphines, and their derivatives have been the most favorite ligands used in amination and cross-coupling reactions due to the readiness of tuning the ligands' electronic and steric character by simply varying their substituents [9–11]. As far as we know little is known about the reaction of Schiff bases with halogenated organophosphorus compounds [12].

In this study the Reaction of biphenylchlorophosphine with (E)-4-((4-bromophenylimino)methyl)benzene-1,2,3-triol have been used to produce the phosphine Schiff base 4-((Z)-(4-bromophenylimino) (diphenylphos-phino)methyl)benzene-1,2,3-triol. This ligand H_3L and its metal complexes **(1-8)** have been fully characterized by different tools. Since phosphine compounds have potential donor sites we have explored its possible complexation by metal ions in order to observe how steric and electronic changes caused by coordination are reflected in variations of chemical and biological properties of the phosphine Schiff base.

2. Experimental

2.1. Syntheses of phosphine Schiff base ligand (H_3L)

A solution of biphenylchlorophosphine (0.001 mole) was added to a well stirred mixture of (E)-4-((4-bromophenylimino)methyl)benzene-1,2,3-triol (0.001 mole) and triethyl amine (TEA) (0.001 mole) in ~ 50 ml dry dioxane. After complete addition the reaction mixture was heated under reflux for seven hours. The solid was formed and filtered off. The filtrate was evaporated under vacuum to give a solid phosphine Schiff base ligand (H_3L) (Figure 1, 2) which was recrystallised from acetone/hexane and dried in a vacuum desiccators.

The creamy white ligand (H_3L). Yield: 76%. Mp: 212 °C. Anal. Calcd (%) for $C_{25}H_{19}BrNO_3P$: C, 60.94; H; 3.89; N; 2.85; P, 6.29. Found: C; 60.99; H;

3.84; N, 2.84; P, 6.28. FT-IR (KBr): 1636 cm^{-1} (vC=N), 1544cm^{-1} (vC-O), 3500 cm^{-1} (vOH), 1450 cm^{-1} (P-aryl). Electronic spectrum: λ_{max} =320 nm, λ_{max} = 464 nm.

2.2. Synthesis of phosphine Schiff base complexes

The metal salts (0.01 mole) dissolved in absolute ethanol (~ 20 ml) was added to appropriate quantity of phosphine Schiff base (0.02 moles) dissolved in absolute ethanol (~30 ml). The mixture was stirred for 3 hours at 60 °C. The precipitate was formed then filtered off, washed with cold ethanol many times and dried in a vacuum desiccator.

The dark brown Cu(II) complex **(1)**. Yield: 90%. Mp: 265 °C. Anal. Calcd (%) for [Cu(L)$_2$(H$_2$O)$_2$]: C, 55.34; H; 3.69; N, 2.58; P, 5.72; Cu, 5.86. Found: C; 55.50; H; 4.01; N, 2.60; P, 5.93; Cu, 6.09. FT-IR (KBr): 1560 cm^{-1} (v_{C-O}), 1620 cm^{-1} ($v_{C=N}$). Electronic spectrum: λ_{max} =350 nm, λ_{max} = 568 nm.

The creamy white Cd(II) complex **(2)**. Yield: 76%. Mp: 289 °C. Anal. Calcd (%) for [Cd(L)$_2$(H$_2$O)$_2$]: C, 53.10; H; 3.54; N, 2.44; P, 5.50; Cd, 9.90. Found: C; 53.60; H; 3.0; N, 2.48; P, 5.40; Cd, 9.94. FT-IR (KBr): 1559 cm^{-1} (v_{C-O}), 1616 cm^{-1} ($v_{C=N}$)

The canary yellow Ti(III) complex **(3)**. Yield: 85 %. Mp: > 360 °C. Anal. Calcd (%) for [Ti(L)$_2$Cl H$_2$O]: C, 55.34; H; 3.53; N, 2.59; P, 5.72. Found: C; 55.40; H; 4.0; N, 2.90; P, 5.70. FT-IR (KBr): 1562 cm^{-1} (v_{C-O}), 1614 cm^{-1} ($v_{C=N}$). Electronic spectrum: λ_{max} = 539 nm.

The pale cream Cr(III) complex **(4)**. Yield: 86%. Mp: > 360 °C. Anal. Calcd (%) for [Cr(L)$_2$Cl H$_2$O]: C, 55.13; H; 3.51; N, 2.55; P, 5.70; Cr, 4.76. Found: C; 55.19; H; 3.52; N, 2.62; P, 5.60; Cr, 4.78. FT-IR (KBr): 1560 cm^{-1} (v_{C-O}), 1621 cm^{-1} ($v_{C=N}$). Electronic spectrum: λ_{max} =279 nm, λ_{max} = 457 nm λ_{max} = 617 nm.

The corral shell Mn(III) complex **(5)**. Yield: 84 %. Mp: > 360 °C. Anal. Calcd (%) for [Mn(L)$_2$(OAC)]: C, 56.87; H; 3.56; N; 2.45; P, 5.65; Mn, 5.0. Found: C; 56.96; H; 3.58; N, 2.55; P, 5.65; Mn, 5.01. FT-IR (KBr): 1563 cm^{-1} (vC-O), 1614 cm^{-1} (vC=N), 653 cm^{-1} δ(OCO). Electronic spectrum: λ_{max} =530 nm, λ_{max} = 605 nm λ_{max} = 743 nm.

The brown Fe(III) complex **(6)**. Yield: 88 %. Mp: > 360 °C. Anal. Calcd (%) for [Fe(L)$_2$Cl H$_2$O]: C, 54.86; H; 3.50; N, 2.53; P, 5.66; Fe, 5.10. Found: C; 55.0; H; 3.51; N, 2.57; P, 5.61; Fe, 5.11. FT-IR (KBr): 1560 cm^{-1} (v_{C-O}), 1616 cm^{-1} ($v_{C=N}$). Electronic spectrum: λ_{max} =448 nm, λ_{max} = 624 nm λ_{max} = 725 nm.

The smoke gray MoO$_2$(VI) complex **(7)**. Yield: 88 %. Mp: > 360 °C. Anal. Calcd (%) for [MoO$_2$(L)$_2$]: C, 54.03; H; 3.24; N, 2.55; P, 5.60. Found: C; 54.80; H; 3.27; N, 2.52; P, 5.58. FT-IR (KBr): 1558 cm^{-1} (v_{C-O}), 1618 cm^{-1} ($v_{C=N}$), 934 cm^{-1} (MoO$_2$).

The golden brown UO$_2$(VI) complex **(8)**. Yield: 80 %. Mp: > 360 °C. Anal. Calcd (%) for [UO$_2$(L)$_2$]: C, 47.85; H; 2.87; N, 2.23; P, 4.90. Found: C; 47.94; H; 2.90; N, 2.24; P, 4.95. FT-IR (KBr): 1561 cm^{-1} (v_{C-O}), 1614 cm^{-1} ($v_{C=N}$).

3. Physical methods

All chemicals used in this study were obtained commercially and used as supplied unless otherwise stated. Bis(acetylacetonato) dioxomolyb-denum(IV) was synthesized according to published procedures [13] and used without further purification. Manganese (III) acetate dihydrate, Chromium chloride hexahydrate, anhydrous ferric chloride, anhydrous titanium trichloride, and uranyl nitrate hexahydrate (S.D.'s fine chemicals) were used for synthesis. Copper acetate monohydrate and cadmium acetate dihydrate were purchased from sigma-Aldrich.

The elemental analyses of C, H, and N were carried out at the Microanalytical Research Center, Faculty of Science, Cairo University. Phosphorus was determined gravimetrically as phosphoammonium molybdate using R. Voy method [14]. IR spectra were obtained using KBr discs (4000-200 cm^{-1}) on a Shimadzu FT- 8201 PC spectrophotometer. UV/VIS spectra were recorded on Perkin EImer Lambda-3B Ultraviolet-Visible spectrophotometer using DMSO or DMF as solvents. ^{13}C NMR spectra were taken on a Varian Mercury 300MHz Em-360-60 MHz instrument. TMS was used as internal standered and deuterated dimethyl sulfoxide as solvent. ^{31}P NMR spectra were run, relative to external H$_3$PO$_4$ (85%), with a varian FT-80 spectrometer at 36.5MHz. Thermogravimetric analysis was performed under a nitrogen atmosphere using a Shimadzu TGA-50H with a flow rate of 20°C min^{-1}. IR, UV/VIS, NMR and thermal analysis were carried out at Cairo University, Cairo, Egypt. Magnetic measurements were recorded by the Gouy method at room temperature using a magnetic susceptibility balance (Johanson Mathey), Alfa product, Model No. (MK). Molar conductances of the phosphorus Schiff base and its transition metal complexes were determined in DMSO (~10^{-3} M) at room temperature using a Jenway Model 4070 conductivity meter. Solid state dc electrical conductivity of the compounds was measured by the two probe method in their compressed pellet form over the 313-403 K temperature range. The Antimicrobial activity was performed using DMF as solvent using agar technique at Fermentation Biotechnology and Applied Microbiology (FERM-BAM) Center, Al-Azhar University, Egypt.

4. Results and discussion

Reaction of biphenylchlorophosphine with (E)-4-((4-bromophenyl-imino)methyl)benzene-1,2,3-triol in presence of triethylamine as a base in dry dioxane readily gives rise to the corresponding 4-((Z)-(4-bromo-phenylimino)(diphenylphosphino)methyl)benzene-1,2,3-triol (H$_3$L) (Figures 1, 2). The reaction of chlorophenylphosphine with imine to form phosphine Schiff base by losing HCl gas and forming P-C bond has been described earlier[15] The product was identified and characterized by its IR, ^{13}C, and ^{31}P NMR spectra. The imine compound prepared by this way is formed in a highly pure and nearly quantitative yield. Reaction of H$_3$L with the metal ions in this study gives the corresponding complexes which are colored and very stable at room temperature in the solid state. The lower yields of the metal complexes than that of the ligand may be due to the steric hindrance around the coordination centre. The ligand and its complexes are soluble in common organic solvents such as CHCl$_3$, EtOH, MeOH, THF, etc. Solution conductivity measurements were performed to establish the charge of the complexes and showed that all compounds are non-electrolyte [16]. The analytical data for the metal complexes indicated 1: 2 metal: ligand stoichiometry.

4.1. Infrared spectra

By comparing the infrared spectra of the ligand (H$_3$L) and its metal complexes, it is found that HL behaves as a bidentate ON donor dibasic ligand. The IR spectrum of the ligand exhibits $v_{C=N}$ (azomethine) and v_{C-O} (phenolic) stretches at 1636 and 1544 cm^{-1}, respectively. The band at 3500 cm^{-1} may be assigned to v_{O-H} stretching. The band at 1450 cm^{-1} range is assigned to the *P*-aryl group [17]. The v_{OH} stretching band in the all metal complexes disappears, as a result of proton substitution by cation coordinated to oxygen. Coordination of the metal ion to phenolic oxygen atom is supported by shifting v_{C-O} (phenolic) band in the complexes to higher wavenumber by ~15 cm^{-1}[18]. A shift of $v_{C=N}$ (azomethine) to a lower energy by 15-22 cm^{-1} in the spectra of the complexes indicates that the coordination takes place through the nitrogen atom. All complexes have a medium and/or weak bands observed in the 510–415 cm^{-1} range attributed to the v_{M-N} and v_{M-O} modes[19].

The IR spectrum of the Mn(II) complex **(5)** displays two bands at 1597 and 1412 cm^{-1} due to $v_{as(OCO)}$ and $v_{s(OCO)}$ modes, respectively. The separation of these two peaks by ~200 cm^{-1} indicates the monodentate coordination of the acetato group to the Mn(II) ion. The band at 653 cm^{-1} is assigned to $\delta_{(OCO)}$, which is considered as a diagnostic band for a monodentate ligand. The MoO$_2$(VI) complex **(7)** exhibits a single band at 934 cm^{-1} due to v_{as}(O=Mo=O) stretching, indicating to the *trans* structure around Mo atom. The spectrum of UO$_2$(II) complex **(8)** shows two bands at 928 and 865 cm^{-1} assigned to v_3 and v_1 vibrations of the O=U=O moiety. The force constant, F for the U=O vibration was calculated and found to be 7.108 m dyn/A° [20]. The U-O bond distance was calculated with the help of the equation [21], $R_{U-O} = 1.08$ F$^{-1/3}$ + 1.17. The bond distance was found to be 1.73 A° which is in the usual range (1.60 - 1.92A°) observed for the majority of the dioxouranium (VI) complexes [20,21]. The presence of coordinated water in the Cu(II), Cd(II), Ti(III), Cr(III), and Fe(III) complexes respectively, is indicated by a broad band at 3453–3368 cm^{-1} and two weaker bands at 843–820 and 725–710 cm^{-1} assigned to the OH rocking and OH wagging vibrations, respectively [22].

In case of the ligand H$_3$L and its metal complexes, it is particularly important to establish whether the molecules retain the imine character of their phenol precursor. The most useful techniques to investigate the tautomeric forms of this ligand are UV and NMR spectroscopy, while IR seems of limited value here because location of the $v_{C=O}$ and v_{C-O} stretches in the spectra is obscured by the abundance of aromatic skeletal modes.

4.2. Electronic, EPR spectra and magnetic moment measurements

The electronic spectra of the ligand H$_3$L and its complexes were recorded in DMF solution in the wavelength range from 200 to 800 nm. Hydrogen-bond forming solvent (DMF) thus favor the formation of the ketoamine. The interaction of enolimine with a hydrogen bond forming solvent would presumably reduce the O–H bond strength and facilitate proton transfer to the nitrogen centre. In like manner, the band in the 464 nm is assigned to the n–π* transition of the azomethine group. In order to investigate the keto-enol tautomeric forms of the free ligand, the electronic spectrum was measured in heptane, chloroform and ethanol. In heptane, the ligand exhibit maxima in 320 nm. However, in chloroform and ethanol, new bands in the 464–337 nm range were observed. The former band at 320 nm in heptane has been assigned to the enolimine and the latter to the ketoamine tautomer of the Schiff base [23].

The electronic spectra of the metal complexes show that, the azomethine chromophore n–π* transition band at 464 nm is shifted to lower frequencies indicating that the imine nitrogen atom is involved in the coordination to the metal ion. The bands at higher energies (~290–206 nm range) are

associated with benzene π–π* transitions. The spectra of the complexes show intense bands in the high-energy region at 302–372 nm which can be assigned to charge transfer L → M bands [24]. Although the precise nature of this transition involving the phenolate group is not fully clear (it has been considered to be an O (phenolate) → metal (II) LMCT [25] or as a metal (II) → π* (phenolate) MLCT [26] transition).

The spectrum of the Ti(III) complex [Ti(L)$_2$Cl H$_2$O] exhibited a broad band at 539 nm due to the $^2T_{2g}$→ ^2E_g transition in an octahedral symmetry which is supported by magnetic moment value of 1.79 B.M. [Cr(L)$_2$Cl H$_2$O] **(4)** exhibits three bands at 617, 457, and 279 nm due to the $^4A_{2g}$→ $^4T_{2g}$, $^4A_{2g}$→ $^4T_{1g}$ and $^4A_{2g}$ →$^4T_{1g}$(P) transitions, respectively, suggesting an octahedral geometry around the Cr(III) ion. This geometry is in accordance with the magnetic moment of 3.86 B.M. The spectrum of the Mn(II) complex [Mn(L)$_2$(OAC)] shows bands at 743, 605, 530 and 353 nm, which can be assigned to the $^5B_1$ →$^5B_2$, $^5B_1$→ $^5A_1$, $^5B_1$ →^5E, and LMCT transitions, respectively. These transitions with the magnetic moment of 4.84 B.M. indicate square-pyramidal structure around Mn(II) ion. The magnetic moment, 5.87 B.M. of the iron (III) complex [Fe(L)$_2$Cl H$_2$O] with the three bands at 725, 624 and 448 nm representing $^6A_{1g}$→ $^4T_{1g}$, $^6A_{1g}$→ $^4T_{2g}$ and $^6A_{1g}$→ ^4E_g transitions, respectively, indicate an octahedral symmetry. The visible spectrum of the UO$_2$ (II) complex in DMSO shows no bands above 500 nm proves that the complex has more than four equatorial groups [27]. The band, observed at 500 nm is attributed to the ^1E_g → $^3\pi_u$ transition [28]. Finally The electronic spectrum of the Cu(II) complex [Cu(L)$_2$(H$_2$O)$_2$] exhibits two bands at 628 nm and 440 nm. These transitions are assignable to $^2B_{1g}$→$^2A_{1g}$ and $^2B_{1g}$→^2E_g respectively. These bands with the magnetic moment 1.86 B.M. which corresponds to one unpaired electron tetragonally distorted octahedral geometry around Cu (II)[29, 30].

The EPR spectral data of copper (II) complex was recorded in polycrystalline states at room temperature. The EPR spectrum (fig. 5) showed that the complex exhibited unresolved signal at high field. This signal is known as an isotropic one with the g∥ closed to 2.22, g⊥ closed to 2.07 and g$_{iso}$ closed to 2.17. These values are characteristic for a d^9 system with an axial symmetry type of d$_{x2-y2}$ ground state. The g values for the copper(II) complexes denote square planar and octahedral geometries around copper(II) ions [31]. Since g∥>g⊥ , thus indicates a tetragonal distortion around the copper (II) ions corresponding to elongation along the four fold symmetry Z-axis. The trend of variation of g values in the order g∥>g⊥>ge (2.0023) showed that the

unpaired electron is localized in the d$_{x2-y2}$ orbital.[32,33] The deviation in the *g*-values from the free electron *g*-value, i.e. 2.0023 is due to the angular momentum contribution in the complexes. The disappearance of hyperfine splitting may be due to higher dipolar and present interactions between the copper (II) ions in the unit cell.

The electronic spectral data, magnetic moment measurements and EPR, IR spectroscopy together with the elemental analysis suggest the proposed structure of the metal complexes (Figure 3).

4.3. ^{13}C and ^{31}P NMR spectral study

Additional structural information can be deduced from the ^{31}P and ^{13}C NMR spectra. The ^{31}P NMR shift recorded for ligand (H$_3$L) shows band at δ 49.066 ppm. This value is in accord with diphenylphosphine shift. The ^{13}C-NMR spectral data (Figure 4) shows bands at δ 142 ppm and δ 160 ppm attributed to imine nitrogen C=N and enolic oxygen C−O respectively. The bands appear at 136 and 140 ppm is in accordance to P-Ar and C-Br respectively. These bands support the authenticity of the proposed structure of the ligand.

5. Solid-state conductivity;

The solid-state dc electrical conductivity of the synthesized ligand H$_3$L and its metal complexes in compressed pellet form (5 ton cm^{-2}) was measured in the temperature range (315–405 K). A linear dependence of log σ = $f(10^3/T)$, as evidence from the Arrhenius plot of electrical conductivity indicates the semiconducting behavior of these compounds [34]. The electrical conductivity (σ) varies exponentially with the absolute temperature according to the relation σ = σ$_o$exp(–E_a/KT), where σ$_o$ is constant, E_a is the activation energy of electrical conduction; T is the absolute temperature, and K is the Boltzmann constant. The dc electrical conductivity values (Table 1) at 40 and 100 °C lie in the range from 7.02 × 10^{-14} to 2.17 × 10^{-11} Ohm^{-1} cm^{-1}. The conductivity of the free ligand is increased on complexing with transition metal ions. This behavior is attributed to the inclusion of the various metal cations in the π-electron delocalization of the ligand[35]. The observed low value of the electrical conductivity can be attributed to low molecular weight of the prepared compounds which lead to low conjugation or undesirable morphology occurs due to pressing the sample into hard brittle pellet form [36].

6. Thermogravimetric analyses

Thermal analyses of the complexes were carried out up to 700°C. All complexes show a gradual mass loss indicating decomposition by fragmentation with the increasing of the temperature. The observed

weight loss obs./calcd. % in the complexes of Ti(III) 1.59/1.66; Cr(III) 1.85/1.65; Fe(III) 1.72/1.65 complexes in the temperature range 185–205 °C corresponds to the loss of one coordinated water molecule, while Cd(II) and Cu(II) complexes show loss of two coordinated water molecules in this temperature range. TG curves show continuous mass loss in the temperature range of 250–650 °C and attain a horizontal level above 650 °C suggesting the formation of the final decomposition product as stable metal oxides. The thermodynamic activation parameters of decomposition processes of the metal complexes namely activation energy (E^*), entropy (ΔS^*) and Gibbs free energy change of the decomposition (ΔG^*) were evaluated graphically by employing three methods, Horowitz–Metzger [37] (HM), Coats–Redfern [38] (CR), and Piloyan–Novikova [39] (PN). Table 2 shows that the entropy change ΔS^* for the formation of the activated complexes from the starting reactants is of positive values. The positive sign of the ΔS^* suggests that the degree of structural (arrangement) of the activated complexes was higher than that of the starting reactants and the decomposition reaction are slow reaction [40].

7. Antibacterial and antifungal activities

The antibacterial activity of the ligand and its metal complexes was evaluated by the Disc diffusion method [41]. The 10-mm diameter Whatmann no. 1 paper discs were soaked in different solutions of the compounds, dried, and then placed in Petri plates previously seeded with the test organism. The plates were incubated for 24 h at 37°C, and the inhibition zone around each disc was measured twice to ensure accuracy. In the present study, all chemically synthesized compounds (the ligand and its metal complexes) were evaluated against Pseudomonas and Klebsiella bacteria and two fungi (A. Niger and A. Flavous). Standard antibiotics namely Gentamicin and standard antifungal drug Nistatin were used for comparison with antibacterial and antifungal activities shown by these compounds, Table 3 (Figure 4) and Table 4 (Figure 5). The metal complexes (**2, 6, 7** and **8**) show a significant activity toward Klebsiella while the complexes (**1, 3** and **4**) are moderately active. On the other hand both ligand and manganese complex show no activity toward this bacterium. The iron (III) complex (**6**) shows less activity toward the Pseudomonas while the titanium (III) complex is found to be a moderately active. The five metal complexes (**1, 2, 4, 7** and **8**) demonstrate significant activity against the Pseudomonas bacterium. Similar to the case of Klebsiella, both of ligand and manganese complex show no activity. The antifungal activities of all complexes were carried out against two fungal strains i.e. A. Niger and A. Flavous and then compared with standard antifungal drug Nistatin (Table 4, Fig. 5). In the whole series, The UO_2(II) complex (**8**) shows the highest inhibition against fungal strain A. Niger and A. Flavus. The ligand and other metal complexes are found to be less active against A. Flavous. On the other hand the ligand together with metal complexes **2, 3, 4** and **5** show moderate activity against A. Niger. The metal complexes **6, 7** and **8** demonstrate a significant activity against A. Niger. The comparison of inhibition zone values for the metal complexes (**1-8**) given in Table 3 (Figure 4) and Table 4 (Figure 5), reveals that the antimicrobial activity could be mainly due to the structure of the complexes and also the oxidation state of the metal ions. A possible explanation for the high toxicity of metal complexes can be explained as follows. The increase in the activity of metal complexes may be due to effect of metal ions on the normal cell process. The polarity of metal ion is considerably reduced on chelation which is mainly because of partial sharing of its positive charge with a donor groups and possibly π-electron delocalization over the whole molecule. Such molecule increases the liphophilic character of the metal complexes which probably leads to breaking down of permeability barrier of the cells resulting in interference with normal cell process [41]. Better activities of the metal complexes compared to free ligand could also be understood in terms of chelation theory, which explains that a decrease in polarizability of the metal could enhance the liphophilicity of the complexes.

8. Conclusion

In this study we have prepared the phosphine Schiff base (H_3L) by reaction biphenylchlorophosphine with (E)-4-((4-bromophenylimino)-methyl) benzene-1,2,3-triol. This ligand and its metal complexes have been fully characterized by different tools such as FT-IR, UV/Visible, ^{13}C, and ^{31}P-NMR, magnetic susceptibility, and conductance measurements. We have explored the possible complexation of the ligand by metal ions in order to observe how steric and electronic changes caused by coordination are reflected in variations of chemical and biological properties of the phosphine Schiff base. Antibacterial and antifungal activities of the ligand and its metal complexes have been investigated. The UO_2 (II) complex demonstrated the highest activity against both of bacteria and fungi used in this study. Better activities of the metal complexes compared to free ligand could be understood in terms of chelation theory.

Table 1: Electrical conductance and some physical properties of HL and its complexes.

Compound no.	Yield (%) [m.p. ($^\circ$C)]	Molecular formula (Formula weight)	$\Lambda_M{}^a$	Electrical conductance	
				$\sigma(40,100°C)$ (Ohm^{-1} cm^{-1})	E_a, eV
H$_3$L	98 / 212	C$_{25}$H$_{19}$BrNO$_3$P (492.30)	-	1.26x10^{-13} / 1.22x10^{-12}	0.263
[Cu(L)$_2$ (H$_2$O)$_2$] (1)	92 / 265	C$_{50}$H$_{40}$Br$_2$CuN$_2$O$_8$P$_2$ (1048.13)	7.6	7.55x10^{-13} / 7.55x10^{-12}	0.186
[Cd(L)$_2$ (H$_2$O)$_2$] (2)	76 / 289	C$_{50}$H$_{40}$Br$_2$CdN$_2$O$_8$P$_2$ (1131.03)	7.8	1.20x10^{-13} / 1.90x10^{-11}	0.554
[Ti(L)$_2$Cl H$_2$O] (3)	90 / >360	C$_{50}$H$_{38}$Br$_2$ClN$_2$O$_7$P$_2$Ti (1083.92)	1.2	1.19x10^{-13} / 1.98x10^{-12}	0.145
[Cr(L)$_2$Cl H$_2$O] (4)	91 / >360	C$_{50}$H$_{38}$Br$_2$ClCrN$_2$O$_7$P$_2$ (1088.05)	7.2	7.04x10^{-14} / 4.87x10^{-13}	0.143
[Mn(L)$_2$(OAC)] (5)	84 / >360	C$_{52}$H$_{39}$Br$_2$MnN$_2$O$_8$P$_2$ (1096.57)	95	4.02x10^{-13} / 4.34x10^{-12}	1.087
[Fe(L)$_2$Cl H$_2$O] (6)	93 / >360	C$_{50}$H$_{38}$Br$_2$ClFeN$_2$O$_7$P$_2$ (1091.90)	1.4	2.55x10^{-13} / 3.44x10^{-12}	0.139
[MoO$_2$(L)$_2$] (7)	88 / >360	C$_{50}$H$_{36}$Br$_2$MoN$_2$O$_8$P$_2$ (1110.52)	7.8	1.24x10^{-13} / 1.89x10^{-12}	0.332
[UO$_2$(L)$_2$] (8)	80 / >360	C$_{50}$H$_{36}$Br$_2$N$_2$O$_8$P$_2$U (1252.61)	9.8	7.04x10^{-13} / 5.67x10^{-12}	0.336

a = (Ω^{-1} cm^2 mol^{-1})

Table 2: Thermal decomposition data of HL and its complexes

Compound.	Half decomp. temp.°C	Activation energy (E_a), KJ/mol (%)			Frequency factor (Z) s^{-1}	Entropy change (ΔS) J/mol K	Free energy change (ΔS) J/mol K
		HM	PN	CR			
H$_3$L	217	13.14	12.98	12.22	2.99x10^{-2}	254.03	195.12
(1) [Cu(L)$_2$ (H$_2$O)$_2$]	376	14.77	14.43	14.65	4.21x10^{-3}	258.44	158.76
(2) [Cd(L)$_2$ (H$_2$O)$_2$]	317	19.27	19.06	18.84	2.55x10^{-2}	254.54	153.64
(3) [Ti(L)$_2$Cl H$_2$O]	368	19.56	19.54	19.23	2.53x10^{-2}	251.56	199.97
(4) [Cr(L)$_2$Cl H$_2$O]	396	17.22	16.75	17.13	4.26x10^{-3}	252.04	188.11
(5) [Mn(L)$_2$(OAC)]	398	17.60	16.97	17.97	9.74x10^{-3}	274.87	198.21
(6) [Fe(L)$_2$Cl H$_2$O]	296	15.12	14.43	14.74	7.08x10^{-4}	255.86	162.45
(7) [MoO$_2$(L)$_2$]	326	13.71	12.53	13.59	5.87x10^{-3}	254.88	204.87
(8) [UO$_2$(L)$_2$]	297	15.12	14.65	15.15	4.12x10^{-3}	259.98	187.77

Table 3: Antibacterial activities of HL and their metal complexes

| Compound	Klebsiella (mm)	Pseudomonas (mm)
H$_3$L	-	-
(1) [Cu(L)$_2$ (H$_2$O)$_2$]	13.25	14.66
(2) [Cd(L)$_2$ (H$_2$O)$_2$]	18.33	15.66
(3) [Ti(L)$_2$Cl H$_2$O]	12.66	12.66
(4) [Cr(L)$_2$Cl H$_2$O]	12.66	17.33
(5) [Mn(L)$_2$(OAC)]	-	-
(6) [Fe(L)$_2$Cl H$_2$O]	14.33	8.00
(7) [MoO$_2$(L)$_2$]	14.66	14.66
(8) [UO$_2$(L)$_2$]	18.00	22.33
Standards Gentamicin	18.00	22.33

5.00 to 8.00 mm are less active, above 10.00 to 13.50 mm are moderately active, 13.50 to 23.33 are significantly active.

Table 4: Antifungal Activities of HL and their metal complexes

Compound	A.Niger (mm)	A.Flavous (mm)
HL	11.00	5.00
(1) [Cu(L)$_2$ (H$_2$O)$_2$]	9.66	7.66
(2) [Cd(L)$_2$ (H$_2$O)$_2$]	12.66	6.00
(3) [Ti(L)$_2$Cl H$_2$O]	10.66	7.00
(4) [Cr(L)$_2$Cl H$_2$O]	11.44	5.44
(5) [Mn(L)$_2$(OAC)]	12.66	7.00
(6) [Fe(L)$_2$Cl H$_2$O]	14.44	6.00
(7) [MoO$_2$(L)$_2$]	14.66	7.00
(8) [UO$_2$(L)$_2$]	29.44	21.66
Standard Nistatin	20.11	21.33

5.00 to 9.00 mm are less active, above 09.00 to 14.00 mm are moderately active, 15.00 to 29.00 are significantly active.
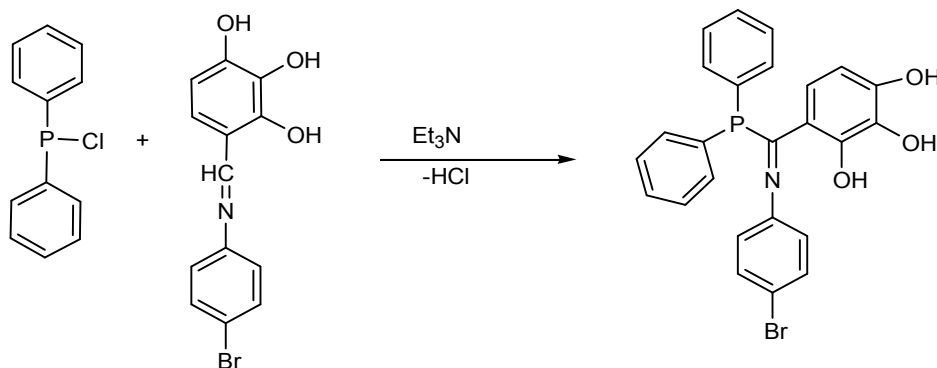
Fig. 1: The proposed structure for H$_3$L ligand.
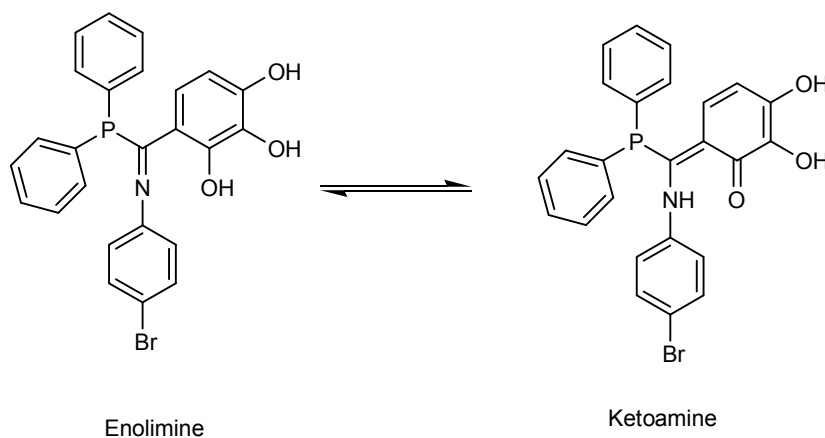
Fig. 2: Tautomeric forms of the H$_3$L ligand.
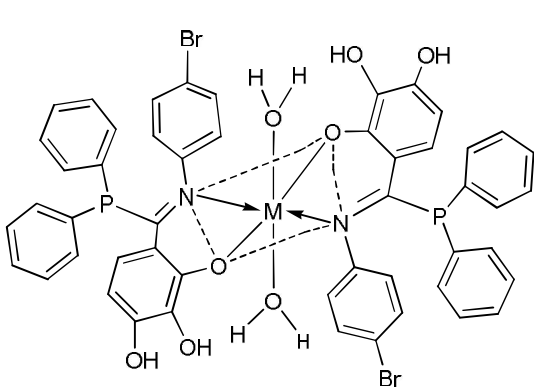
M = Ti(III) **(3)**, Cr(III) **(4)**, and Fe(III) **(6)**
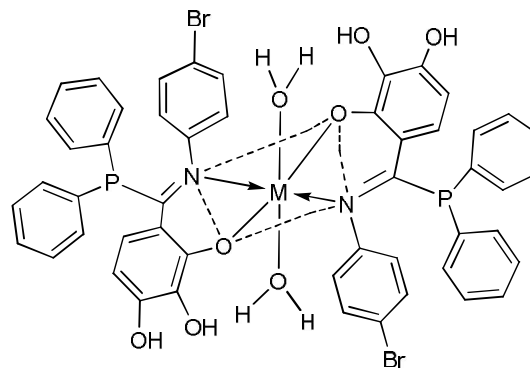
M =Cu(II) **(1)**, and Cd(II) **(2)**
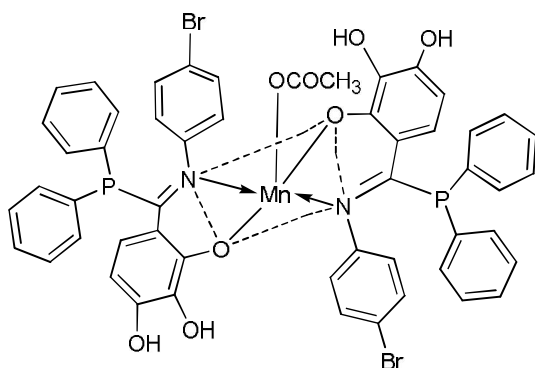
(5)
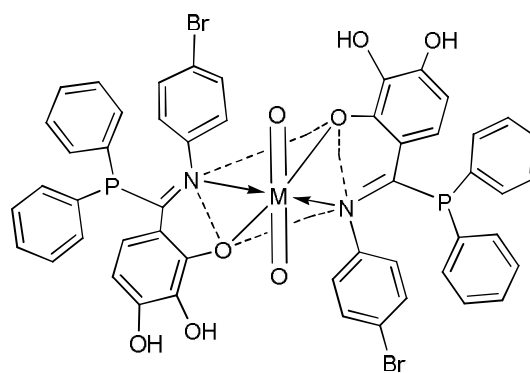
M = Mo(II) **(7)**, and U(II) **(8)**

Fig. 3: The proposed structures of H₃L complexes.
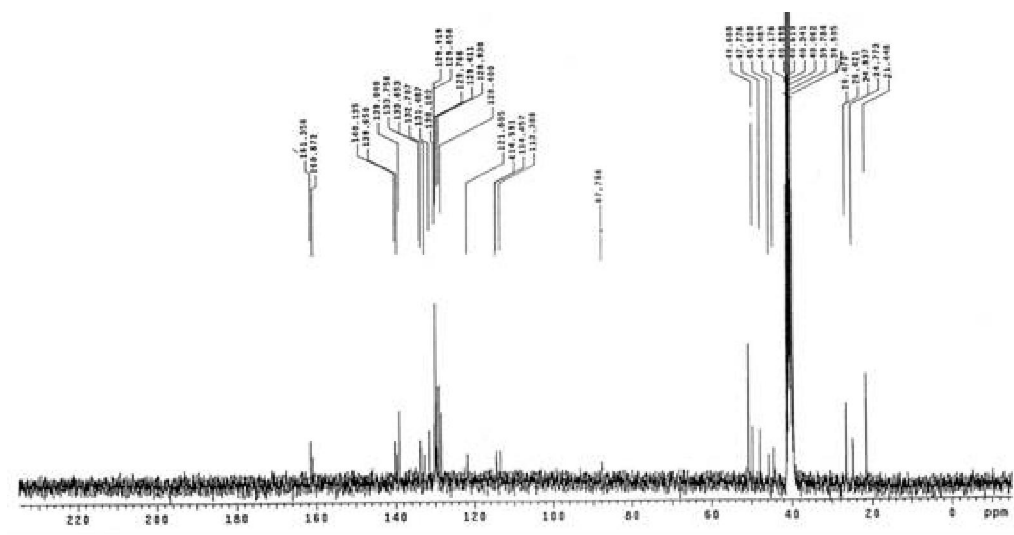
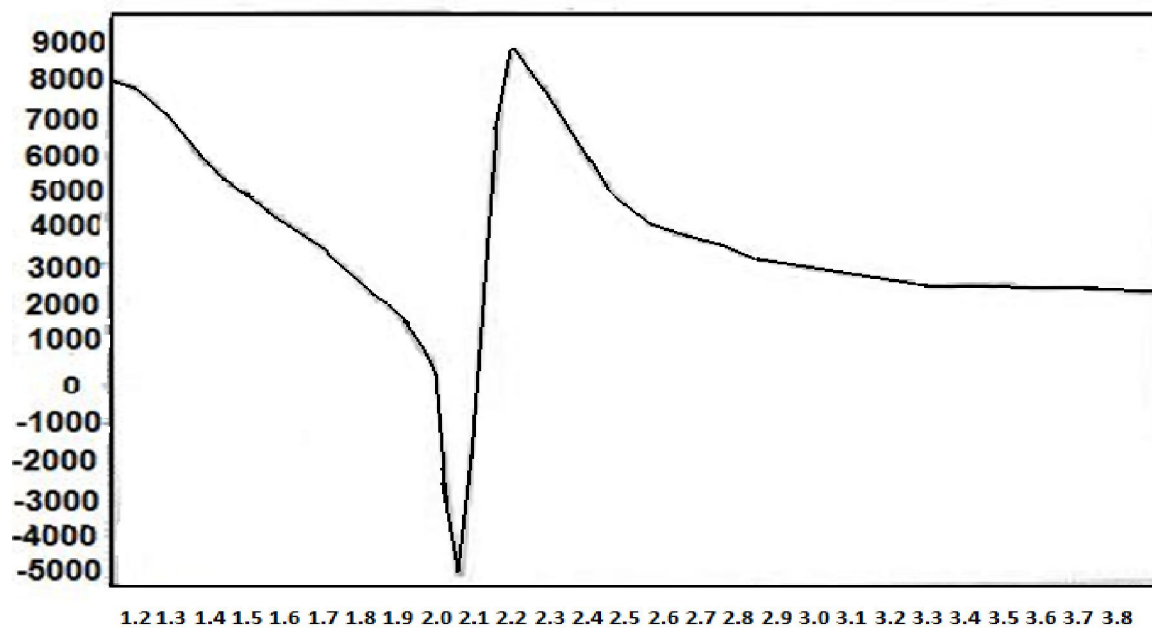Fig. 4: ^{13}C nmr of the ligand (H₃L).

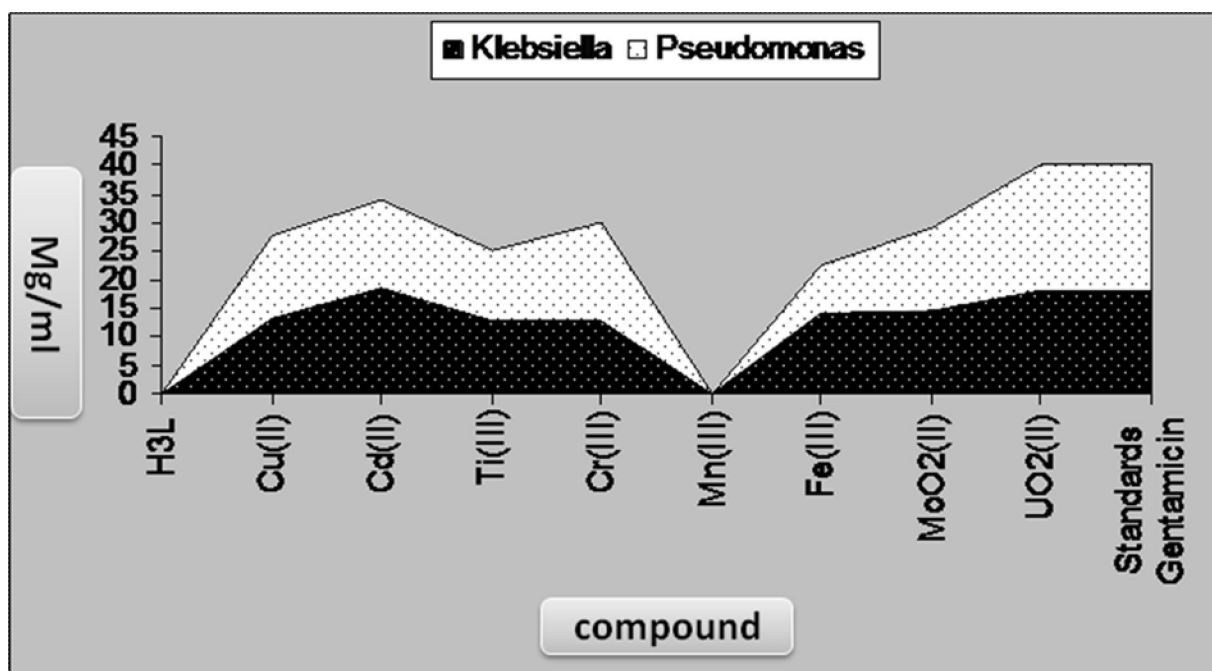Fig. 5: EPR spectrum of the copper complex [Cu(L)$_2$ (H$_2$O)$_2$].

Fig. 6: MICs of the ligand and their metal complexes against bacteria (MIC values were determined as mg/mL active compounds in medium).
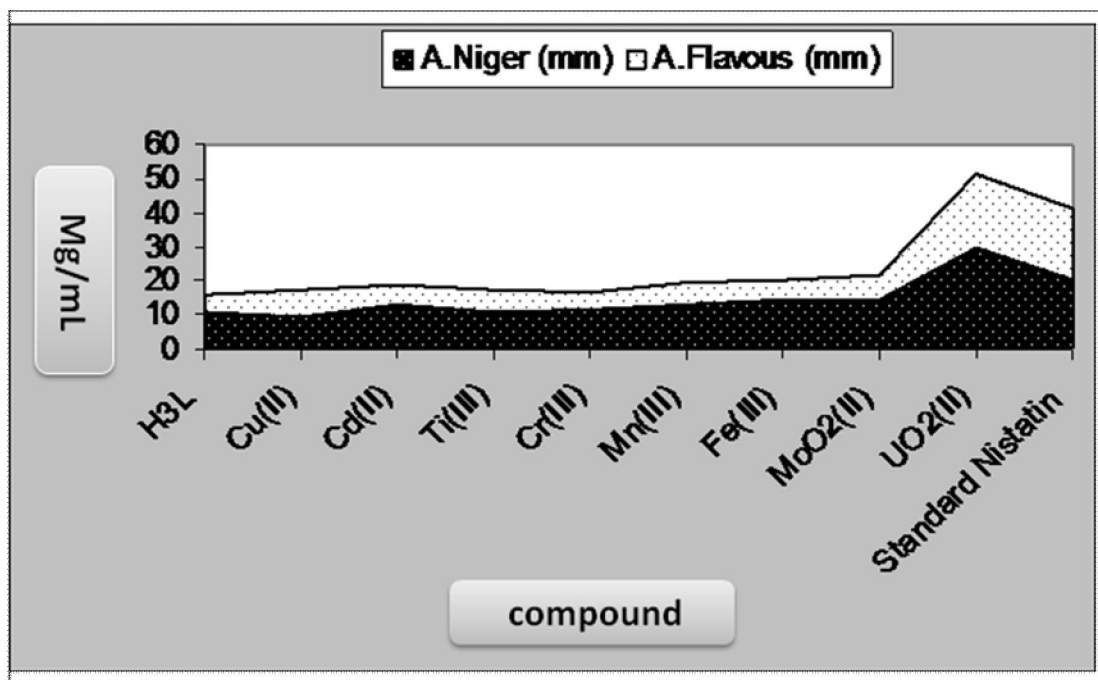
Fig. 7: MICs of the ligand and their metal complexes against fungi (MIC values were determined as mg/mL active compounds in medium).

References

[1] Aminabhavi, T.M.; Biradar, N.S.; Divarar, M.C.; *Ind. J. Chem. A.* **25**, 482, (1986).

[2] Tarafladar, M.T.H.; *Ind. J. Chem. Soc.* **28**, 531, (**1989**).

[3] Blake, A.J.; Mcinnes, J.M.; Mountford, P.; *J. Chem. S, Bull. Chem. Soc. Dalton Trans.* **379**, (1999).

[4] Tümer, M.; Köksal, H.; Sener, M.K.; Serin, S.; *Trans. Met. Chem.* **24**, 414 (1999).

[5] Pyrz, J.W.; Roe, A.I.; Stern, L.J.; Que, J.R.; *J. Am. Chem. Soc.* **107**, 614, (1985).

[6] Zishen, W.; Zhiping, L.; Zhenhuan, Y.; *Trans. Met. Chem.* **18**, 291, (1993).

[7] Chakraborty, J.; Patel, R.N.; *J. Ind. Chem. Soc.* **73**, 191, (1996).

[8] Farag, R.S.; El-Sayed, B.A.; El-Nawawy, M.A.; Shaaban, S.M.; *Phosphorus, Sulfur, and Silicon,* **179**, 1923, (2004).

[9] Tang, W.; Zhang, X.; *Chem. Rev.* **103**, 3029, (2003).

[10] Andersen, N.G.; Keay, B.A.; *Chem. Rev.* **101**, 997, (2001).

[11] Planas, J.G.; Gladysz, J.A.; *Inorg. Chem.* **41**, 6947, (2002).

[12] Wolf, J.; Labande, A.; Daran, J.; Poli, R.; *J. Organomett. Chem.* **691**, 433, (2006).

[13] Christensen, O.T.; *Inorg. Chem.* **27**, 325, (1901).

[14] Voy, R.; *Chem. Ztg. Chem. Appratus* **21**, 441, (1897).

[15] Alaghaz, A.M.A.; Ammar, R.A.; *Eur. J. of Med. Chem.* **45,** 1314 (2010).

[16] Alaghaz, A.M.A.; Ammar, R.A.; *J. Phosphorus, Sulfur, and Silicon, and the Related Elements,* **183**, 2827, (2008).

[17] Soliman, F.M.; Said, M.M.; Maigali, S.S.; *Monatshefte für Chemie,* **136**, 241, (2005).

[18] Geary, W.J.; *Coord. Chem. Rev.* **7**, 81, (1971).

[19] Tümer, M.; Celik, C.; Köksal, H.; Serin, S.; *Trans. Met. Chem.* **24**, 525, (1999).

[20] McGlynn, P.; Smith, J.K.; Neely, W.C.; *J.Mol. Spect.* **6**, 164, (1961).

[21] Jones, L.J.; *Spectrochim. Acta,* **10**, 395, (1958).

[22] Singh, G.; Singh, A.; Singh, K.; *Proc. Nat. Acad. Sci.* **72**, 87, (2002).

[23] Dolaz, M.; Tümer, M.; Dığrak, M.; *Trans. Met. Chem.* **29**, 528, (2004).

[24] Amundsen, A.R.; Whelan, J.; Bosnich, B.; *J. Am. Chem. Soc.* **99**, 6730, (1977).

[25] Tümer, M.; *Synth. React. Inorg. Met. Org. Chem.* **30**, 1139, (2000).

[26] Atkins, R.; Brewer, G.; Kokot, E.; Mockler, G.M.; Sinn, E.; *J. Inorg. Chem.* **24**, 127, (1985).

[27] Bhattacharya, R.G.; Bera, D.C.; *J. Ind. Chem. Soc.* **52**, 375, (1975).

[28] Addison, C.C.; Champ, H.A.J.; Hodge, N.; Norbury, A.H.; *J. Chem. Soc.* **2354**, (1964).

[29] Lever, A.B.P.; *Inorganic Electronic Spectroscopy, second ed., Elsevier, Amsterdam,* 1984.

[30] Chandra, S.; Gupta, L.K.; *Spectrochim. Acta A,* **60**, 2767, (2004).

[31] El-Tabl, A.S.; *Trans. Met. Chem.* **22**, 166, (2002).

[32] Chandra, S.; Gupta, L. K.; *Spectrochim. Acta Part A,* **62**, 1102, (2005).

[33] Chandra, S.; Gupta, L. K.; *Spectrochim. Acta Part A,* **60**, 2411, (2004).

[34] Srivastava, R.S.; *Inorg. Chem. Acta*, **56**, 165, (1981).

[35] Alaghaz, A.M.A; *J. Phosphorus, Sulfur, and Silicon, and the Related Elements,* **183**, 2807, (2008).

[36] Aswar, A.S.; Mohod, R.B.; Bhadange, S.G.; *Ind. J. Chem.* **40**, 1110, (2001).

[37] Horowitz, H.H.; Metzger, G.; *J. Anal. Chem.* **1954**, (1963).

[38] Coats, A.W;. Redfern, J.P.; *Nature,* **201**, 68, (1964).

[39] Piloyan, G.O.; Pyabonikar, T.D.; Novikova, C.S.; *Nature,* **212**, 1229, (1966).

[40] Valaev, L.T.; Gospodinov, G.G.; *Thermochim. Acta*, **370**, 15, (2001).

[41] Srivastava, R.S.; *Inorg. Chim.Act.* **56**, 65, (1981).

12/12/2011